Analyzing imprecise graphene foam resistance data

Materials Research Express

OPEN ACCESS

RECEIVED
17 February 2022

REVISED
28 March 2022

ACCEPTED FOR PUBLICATION
1 April 2022

PUBLISHED
20 April 2022

PAPER

Analyzing imprecise graphene foam resistance data

Usama Afzal[1,*], **Muhammad Aslam**[2] **and Ali Hussein AL-Marshadi**[2]

[1] Department of Physics, University of Education, Township Campus, Lahore 54000, Pakistan
[2] Department of Statistics, Faculty of Science, King Abdulaziz University, Jeddah 21551, Saudi Arabia
[*] Author to whom any correspondence should be addressed.

E-mail: mohammadusamafzal7@gmail.com, aslam_ravian@hotmail.com and aalMarshadi@kau.edu.sa

Keywords: graphene foam, Ni foam, XRD

Abstract

3D graphene foam is the main aim of this research work. Graphene foam is synthesized on the Ni-foam by the CVD technique. The graphene foam has been characterized by XRD, FESEM, Raman spectroscopy and BET techniques. The resistance of graphene foam with a variance of temperature has been measured through an LCR meter and has been analyzed with classical and neutrosophic analysis. As a result, it is seen that graphene foam is expressing both conductor and semiconductor electric properties and also it is observed that neutrosophic analysis is more flexible to analyze the resistance of graphene foam.

1. Introduction

The development of flexible electronic circuits and devices has increased dramatically in recent years. Numerous nano-materials are used for this purpose like carbon containing-materials i.e. carbon nano-tubes (CNTs) and carbon nano-fibers, see (Zhang *et al* 2015) and (Dimchev *et al* 2010). Graphene is a chemically derived nanomaterial, which is an allotropic form of carbon with 2D hexagonal lattices and has zero band gaps, see (Geim & Novoselov, 2010). It has remarkable electric and conducting properties like it has 4 times larger electron mobility than III-V, see (Chen *et al* 2008). Numerous researchers have worked to connect 2D graphene with 3D structure materials by exploiting graphene foam, for remarkable electrical and thermal properties, which can be used in different applications, see (Geim 2009). Generally, it is seen that graphene foam is produced by chemical vapor deposition (CVD). The microcellular graphene foam based on Ni foam was fabricated with the help of ambient pressure CVD, which has a pore wall thickness of 5 nm (Jiang *et al* 2016). Similarly, the synthesization of 3D graphene foam with higher electrical conductivity of about 125 S cm^{-1} with a surface area of about 1625.4 cm g^{-1}, was performed by plasma-enhanced CVD (Chen *et al* 2014). Also, CVD is used to fabricate the graphene foam based on Ni nanowires for high electric and mechanical properties (Min *et al* 2014). The reference (Jinlong *et al* 2017) used pitting pits Ni foam to fabricate the 3D graphene foam. They used NaCl solution to create pitting pits on the surface of Ni foam and deposited the graphene by CVD. The reference (Li *et al* 2015) developed the graphene foam through the graphene oxide (GO) on Ni foam and used it for sensing purposes. Also, different researchers have worked on graphene foams and got useful data of their electric, thermal as well as mechanical properties. The analysis of this data is a very caring task that is performed in form of tables as well as graphs through different methods like the classical analysis. More information can be seen in (Huang *et al* 2017).

Neutrosophic is a type of method used to analyze the data, which was introduced by Smarandache (Smarandache 2013). It is a reliable technique of statistics, which is the generalization of the fuzzy technique and is also more efficient. At the present time, the use of neutrosophic techniques is increased to analyze the data in several fields i.e. in medicine for diagnoses data measurement (Ye 2015), in applied sciences (Christianto *et al* 2020), in astrophysics i.e. earth speed (Aslam, 2021a), in humanistic (Smarandache 2010) and in material science (Afzal *et al* 2021, 2021). The neutrosophic technique is used on the interval point values data i.e. having indeterminacy, see (Aslam 2021b). This is a significant benefit over the classical techniques because classical statistics only deal with fixed point values data i.e. having no indeterminacy. Moreover, the neutrosophic

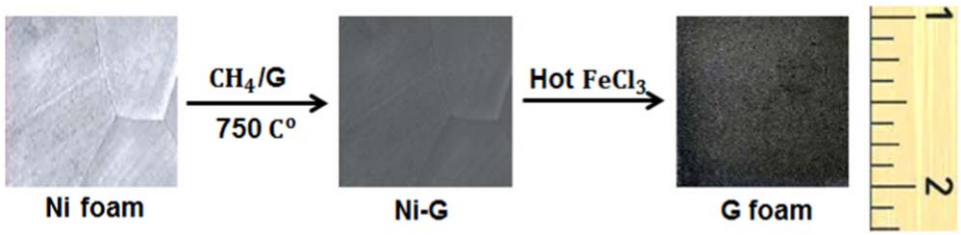

Figure 1. Graphene foam of size 23 × 23 mm.

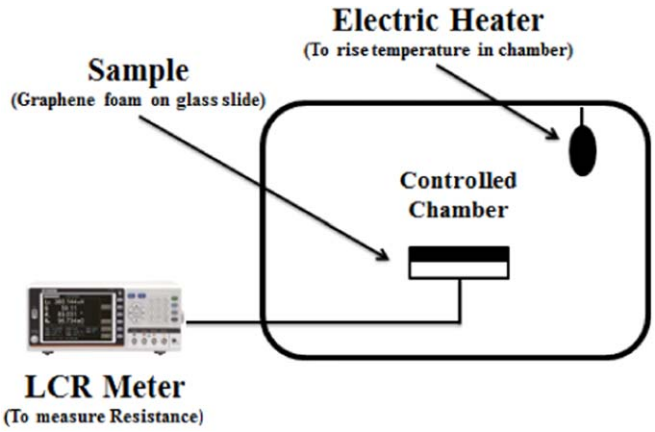

Figure 2. Schematic diagram of characterization setup.

technique is more helpful than classical techniques see the examples in the following references (Smarandache 2014, Chen *et al* 2017a, 2017b). Different statistical techniques were developed under neutrosophic statistics by Muhammad Aslam (Aslam 2020a, 2020b).

Present work reports the motive study of graphene foam resistance variance due to changes in temperature and current. Graphene foam is produced on the Ni foam surface through CVD and its structural, as well as morphological properties, are investigated with different characterization techniques. The resistance of the foam is measured with respect to the temperature as well as current and analyzed through neutrosophic as well as the classical analysis methods.

2. Experimental

For the fabrication of the GF, we have used porous nickel (pure 99.99%) foam of size about 25 × 25 mm as the template for graphene deposition as shown in figure 1. The Ni foam is first cleaned with the by sonication in acetone for 2 h, then put in DI water for 30 min and dried by oven at 100 °C for 5 h. The Chemical vapor deposition (CVD) technique with a decomposition of CH_4 at 750 °C under ambient pressure has been used for the deposition of graphene on Ni foam. A hot $FeCl_3$ solution has been used to remove the Ni and as a result, we have gotten the 3D graphene foam structure (Yavari *et al* 2011).

Then, we put this graphene foam on a clean glass slide for the characterization of structure, electric and surface properties. For structural properties XRD and for surface morphology FESEM techniques have been used. Raman spectroscope having a laser excitation with 488 nm wavelength has been used to observe the quality of 3D graphene foam. Similarly, to observe the adsorption of nitrogen gas on the surface area of 3D graphene foam the Brunauere-Emmette-Teller (BET) has been also used. The electric properties by measuring resistance are studied in the lab at room temperature. For measuring the resistance of the sample LCR meter has been used which is associated with a controlled chamber as shown in figure 2. Resistance is measured by varying the temperature and current, separately. All data has been collected in interval form i.e. at any specific value of temperature or current both maximum and minimum change in the value of resistance has been measured for analysis by both classical and neutrosophic approach.

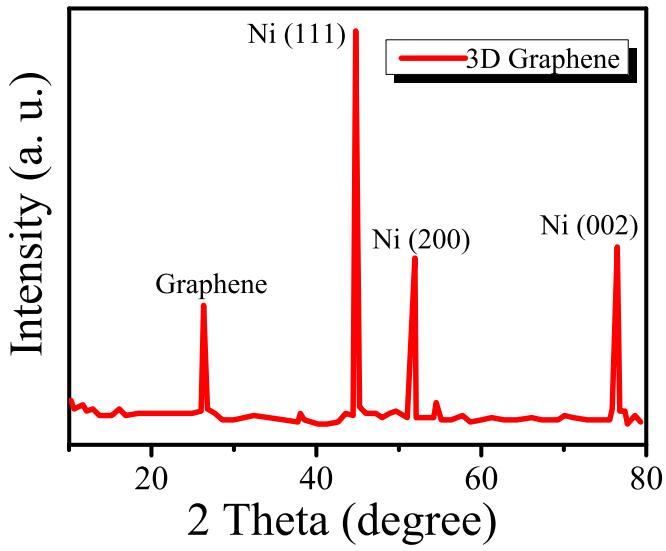

Figure 3. XRD Pattern of graphene foam.

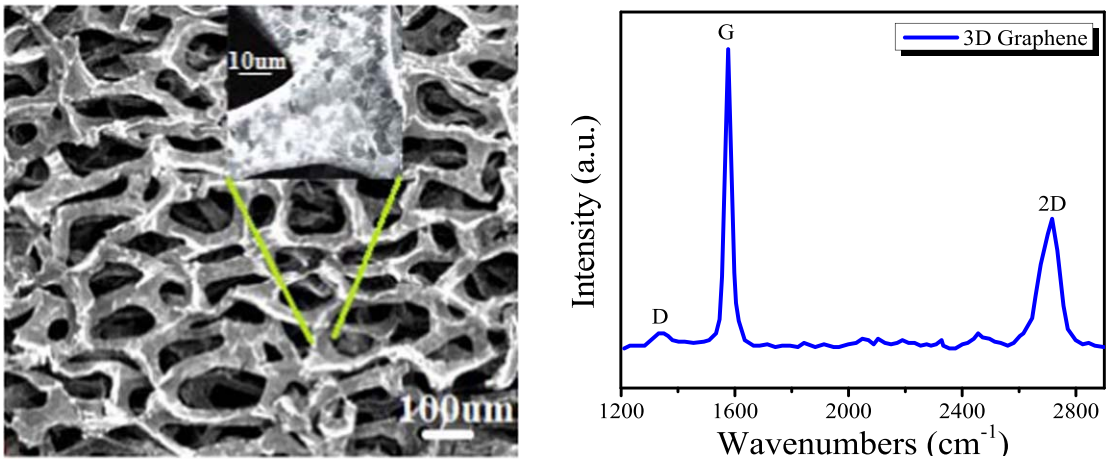

Figure 4. Lift side is the FESEM of the graphene foam on Ni foam and Right side is the Raman shift of the graphene foam.

3. Result and discussion

XRD patterns of graphene foam can be seen in figure 3. All the peaks are satisfying the standard value. The first peak at 26.1° is expressing the presence of graphene. It is seen that the peak of graphene is shifted down slightly i.e. not much sharper, which is indicating that the interlayers of graphene with d002 spacing decrease based on Bragg's law, see (Ebrahimi *et al* 2019, Yang and Guo 2019). Similarly, (111) at 44.8°, (200) at 52.1° and (002) at 76.9° peaks are expressing the existence of the Ni foam.

The surface morphology of the graphene foam has been analyzed through field emission scanning electron microscopy (FESEM) as shown in figure 4(lift side). There are many black spots which are expressing the Ni foam and also 3D graphene structure on Ni foam can be easily seen. It is also observed that the morphology of the graphene is not changed and exhibits gauze morphology with wrinkles and ripples edge. It is assumed that wrinkles and ripples of graphene could be led to lower free energy in the system and avoid the graphene combinations to stabilize the graphene interlayers structure (Fasolino *et al* 2007).

Similarly, figure 4 (right side)is expressing the Raman spectroscopy spectrum. We have observed three peaks as D, G and 2D at the wavenumbers about 1370, 1591 and 2695 cm^{-1}, respectively. The 'D' is a defect peak, which is highlighting the defects as well as disorders between layers of graphene. The 'G' is the characteristic peak of carbon structure sp^2, which is highlighting the symmetry as well as the crystallization of graphene structure. Similarly, '2D' is a double-phonon-resonance peak, which is expressing the graphene stack degree i.e. identifying the presentence of graphene, see (Ferrari *et al* 2006, Qin *et al* 2022). We have used the BET technique to observe the specific surface area of the 3D graphene. We have calculated about 411.95 m^2/g specific surface

Table 1. Resistance measured data by changing temperature and current.

Temperature (K)	Resistance (Ω)	Current (mA)	Resistance (Ω)
292	[3.025; 3.047]	1	[3.013, 3.025]
296	[3.010; 3.031]	5	[3.001, 3.009]
301	[2.998; 3.020]	10	[3.000, 3.008]
305	[2.992; 3.017]	15	[2.991, 3.010]
309	[2.980; 3.002]	20	[2.986, 3.001]
315	[2.971; 2.992]	25	[2.984, 2.995]
319	[2.981; 3.002]	30	[2.976, 2.992]
323	[2.975; 2.997]	35	[2.972, 2.988]
328	[2.967; 2.988]	40	[2.964, 2.983]
331	[2.971; 2.991]	45	[2,955, 2.971]
335	[2.967; 2.987]	50	[2.945, 2.966]
339	[2.957; 2.978]	55	[2.943, 2.952]
345	[2.935; 2.958]	60	[2.942, 2.961]
353	[2.925; 2.947]	65	[2.941, 2.956]
360	[2.914; 2.935]	70	[2.932, 2.946]
366	[2.912; 2.933]	75	[2.925, 2.936]
375	[2.903; 2.925]	80	[2.912, 2.936]
378	[2.891; 2.914]	85	[2.910, 2.926]
383	[2.892; 2.915]	90	[2.906, 2.918]
388	[2.895; 2.917]	95	[2.902, 2.920]
393	[2.891; 2.913]	100	[2.899, 2.916]
398	[2.880; 2.901]	105	[2.895, 2.913]
405	[2.859; 2.881]	110	[2.892, 2.908]
412	[2.857; 2.880]	115	[2.889, 2.902]
419	[2.844; 2.867]	120	[2.888, 2,901]
426	[2.841; 2.862]	125	[1.880, 2.895]
431	[2.830; 2.854]	130	[2.879, 2.893]
435	[2.837; 2.859]	135	[2.869, 2.888]
449	[2.820; 2.842]	140	[2.862, 2.883]

area of graphene foam. That is expressing the high porosity with a high surface area of the graphene foam. This means that graphene is very advantageous for contacting the electrodes materials, used in the electrochemical systems and electric layers for different devices like capacitors, see (Zhang and Zhao 2009, Yan *et al* 2019, Qi *et al* 2021) etc. One can also find the electrochemical impedance test using the EIS as expressed in the following reference (Yan *et al* 2022). But we have not added this work due to the unavailability of technique.

We have fabricated the sample according to (Yavari *et al* 2011, Jiang *et al* 2016, Jinlong *et al* 2017) and we used an LCR meter to measure the electrical properties of the graphene foam. We noted that data is imprecise (i.e. it is in intervals) and reported the graphene foam measurement obtained from the LCR meter in table 1. For the data in the interval, neutrosophic statistics can be applied effectively as compared to classical statistics.

From the above table 1, it is seen that the resistance of the graphene foam on Ni foam decrease with an increase in the temperature and current. This is because the graphene is a zero-gap semiconductor; the initial value of temperature resistance is a maximum but as the temperature increases the charge carrier's density also increases, so resistance starts to decrease. However, the resistance is not smoothly decreasing. Because for graphene foam the graphene is deposed on the Ni foam and Ni is a conductor in nature. Similarly, for current same thing happens. In short, the graphs are expressing the major semiconductor and minor conductor properties of the graphene foam.

3.1. Analysis of resistance of graphene foam

As already mentioned, we have performed two types of analysis i.e. classical and neutrosophic analysis. For the classical analysis, we take the average [(maximum value + minimum value)/2] of the interval to convert the interval value into a fix point value. For example, at 292 K temperature, we get [3.025; 3.047] Ω resistance interval. So, we convert it into a fix point value i.e. 3.036 Ω by taking its average. But for neutrosophic analyses, we have to first develop or modify the neutrosophic formula, so let us see the definition of neutrosophic.

Let if $A_N \in [A_L, A_U]$ is the random value variable with indeterminacy interval $I_N \in [I_{NL}, I_{NU}]$, then the neutrosophic formula is written as follows:

Table 2. Classical analysis of resistance of graphene foam.

Temperature (K)	Resistance (Ω)	Current (mA)	Resistance (Ω)
292	3.036	1	3.019
296	3.0205	5	3.005
301	3.009	10	3.004
305	3.0045	15	3.0005
309	2.991	20	2.9935
315	2.9815	25	2.9895
319	2.9915	30	2.984
323	2.986	35	2.98
328	2.9775	40	2.9735
331	2.981	45	2.963
335	2.977	50	2.9555
339	2.9675	55	2.9475
345	2.9465	60	2.9515
353	2.936	65	2.9485
360	2.9245	70	2.939
366	2.9225	75	2.9305
375	2.914	80	2.924
378	2.9025	85	2.918
383	2.9035	90	2.912
388	2.906	95	2.911
393	2.902	100	2.9075
398	2.8905	105	2.904
405	2.87	110	2.9
412	2.8685	115	2.8955
419	2.8555	120	2.8945
426	2.8515	125	2.8875
431	2.842	130	2.886
435	2.848	135	2.8785
449	2.831	140	2.8725

$$A_{iN} = A_{iL} + A_{iU} I_N \ (i = 1, 2, 3, \ldots, n_N) \tag{1}$$

The size of the neutrosophic variable is $n_N \epsilon [n_{NL}, n_{NU}]$. The variable $A_{iN} \epsilon [A_{iL}, A_{iU}]$ has two parts: a lower value A_{iL} a classical part and an upper value $A_{iU} I_N$ an indeterminate part having an indeterminacy interval $I_N \epsilon [I_{NL}, I_{NU}]$.

Similarly, the neutrosophic mean $\bar{A}_N \in [\bar{A}_L, \bar{A}_U]$ is defined as follows:

$$\bar{A}_N = \bar{A}_L - \bar{A}_U I_N; \ I_N \in [I_L, I_U] \tag{2}$$

Now let us use these preliminaries for developing the neutrosophic formula for the present condition. As the resistance of the graphene foam depends on the variation of temperature (T) and current (I) so we can write it as the function of them i.e. $R(T)$ and $R(I)$. So, the neutrosophic formula is written as (Afzal *et al* 2021):

$$R(T)_N = R(T)_L + R(T)_U I_N; \ I_N \in [I_L, I_U] \tag{3}$$

The above resistance formula $R(T)_N \in [R(T)_L, R(T)_U]$ is an extension under the classically. The equation is containing two parts i.e. $R(T)_L$ determined & $R(T)_U I_N$ indetermined parts. Moreover, $I_N \in [I_L, I_U]$ is known as an indeterminacy interval. Also, the measured resistance interval $R(T)_N \in [R(T)_L, R(T)_U]$ can be reduced to the classical or determined part if we choose $I_L = 0$ and I_U can be calculated by $(R(T)_U - R(T)_L)/R(T)_U$.

For example, we have observed the first interval value of resistance [3.025; 3.047] Ω at 292 K temperatures. Here $R(T)_L$ is 3.025 and $R(T)_U$ is 3.047. Similarly, indeterminacy $I_L = 0$ as a reason has been mentioned above and I_U is 0.0073. The neutrosophic approach for the above interval is written as:

$$R(T)_N = 3.025 + 3.047IN; \ I_N \in [0, 0.007] \tag{4}$$

Similarly, for R(I) the neutrosophic formula can be written:

$$R(I)_N = R(I)_L + R(I)_U I_N; \ I_N \in [I_L, I_U] \tag{5}$$

By following the above procedure we have analyzed data and plotted the graphs. Classical analysis of resistance with respect to temperature and with respect to current variance is shown in table 2 and neutrosophic analysis is in table 3:

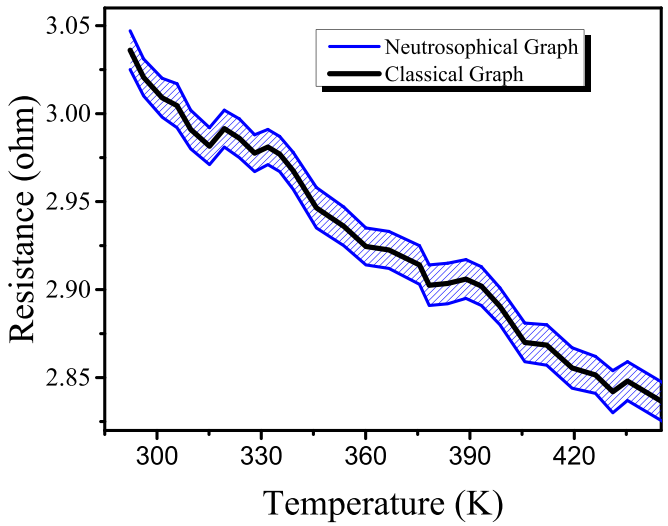

Figure 5. Graphs of resistance versus temperature for graphene foam.

Table 3. Classical analysis of resistance of graphene foam.

Temperature (K)	Resistance (Ω)	Current (mA)	Resistance (Ω)
292	$3.025 + 3.047I_N;\ I_N \in [0,\ 0.007]$	1	$3.013 + 3.025I_N;\ I_N \in [0,\ 0.004]$
296	$3.010 + 3.031I_N;\ I_N \in [0,\ 0.007]$	5	$3.001 + 3.009I_N;\ I_N \in [0,\ 0.003]$
301	$2.998 + 3.020I_N;\ I_N \in [0,\ 0.007]$	10	$3.000 + 3.008I_N;\ I_N \in [0,\ 0.003]$
305	$2.992 + 3.017I_N;\ I_N \in [0,\ 0.008]$	15	$2.991 + 3.010I_N;\ I_N \in [0,\ 0.006]$
309	$2.980 + 3.002I_N;\ I_N \in [0,\ 0.007]$	20	$2.986 + 3.001I_N;\ I_N \in [0,\ 0.005]$
315	$2.971 + 2.992I_N;\ I_N \in [0,\ 0.007]$	25	$2.984 + 2.995I_N;\ I_N \in [0,\ 0.004]$
319	$2.981 + 3.002I_N;\ I_N \in [0,\ 0.007]$	30	$2.976 + 2.992I_N;\ I_N \in [0,\ 0.005]$
323	$2.975 + 2.997I_N;\ I_N \in [0,\ 0.007]$	35	$2.972 + 2.988I_N;\ I_N \in [0,\ 0.005]$
328	$2.967 + 2.988I_N;\ I_N \in [0,\ 0.007]$	40	$2.964 + 2.983I_N;\ I_N \in [0,\ 0.006]$
331	$2.971 + 2.991I_N;\ I_N \in [0,\ 0.007]$	45	$2.955 + 2.971I_N;\ I_N \in [0,\ 0.005]$
335	$2.967 + 2.987I_N;\ I_N \in [0,\ 0.007]$	50	$2.945 + 2.966I_N;\ I_N \in [0,\ 0.007]$
339	$2.957 + 2.978I_N;\ I_N \in [0,\ 0.007]$	55	$2.943 + 2.952I_N;\ I_N \in [0,\ 0.003]$
345	$2.935 + 2.958I_N;\ I_N \in [0,\ 0.008]$	60	$2.942 + 2.961I_N;\ I_N \in [0,\ 0.007]$
353	$2.925 + 2.947I_N;\ I_N \in [0,\ 0.008]$	65	$2.941 + 2.956I_N;\ I_N \in [0,\ 0.005]$
360	$2.914 + 2.935I_N;\ I_N \in [0,\ 0.007]$	70	$2.932 + 2.946I_N;\ I_N \in [0,\ 0.005]$
366	$2.912 + 2.933I_N;\ I_N \in [0,\ 0.007]$	75	$2.925 + 2.936I_N;\ I_N \in [0,\ 0.004]$
375	$2.903 + 2.925I_N;\ I_N \in [0,\ 0.008]$	80	$2.912 + 2.936I_N;\ I_N \in [0,\ 0.008]$
378	$2.891 + 2.914I_N;\ I_N \in [0,\ 0.008]$	85	$2.910 + 2.926I_N;\ I_N \in [0,\ 0.005]$
383	$2.892 + 2.915I_N;\ I_N \in [0,\ 0.008]$	90	$2.906 + 2.918I_N;\ I_N \in [0,\ 0.004]$
388	$2.895 + 2.917I_N;\ I_N \in [0,\ 0.008]]$	95	$2.902 + 2.920I_N;\ I_N \in [0,\ 0.006]$
393	$2.891 + 2.913I_N;\ I_N \in [0,\ 0.008]$	100	$2.899 + 2.916I_N;\ I_N \in [0,\ 0.006]$
398	$2.880 + 2.901I_N;\ I_N \in [0,\ 0.007]$	105	$2.895 + 2.913I_N;\ I_N \in [0,\ 0.006]$
405	$2.859 + 2.881I_N;\ I_N \in [0,\ 0.008]$	110	$2.892 + 2.908I_N;\ I_N \in [0,\ 0.006]$
412	$2.857 + 2.880I_N;\ I_N \in [0,\ 0.008]$	115	$2.889 + 2.902I_N;\ I_N \in [0,\ 0.005]$
419	$2.844 + 2.867I_N;\ I_N \in [0,\ 0.008]$	120	$2.888 + 2,\ 901I_N;\ I_N \in [0,\ 0.005]$
426	$2.841 + 2.862I_N;\ I_N \in [0,\ 0.007]$	125	$1.880 + 2.895I_N;\ I_N \in [0,\ 0.005]$
431	$2.830 + 2.854I_N;\ I_N \in [0,\ 0.009]$	130	$2.879 + 2.893I_N;\ I_N \in [0,\ 0.005]$
435	$2.837 + 2.859I_N;\ I_N \in [0,\ 0.008]$	135	$2.869 + 2.888I_N;\ I_N \in [0,\ 0.007]$
449	$2.820 + 2.842I_N;\ I_N \in [0,\ 0.008]$	140	$2.862 + 2.883I_N;\ I_N \in [0,\ 0.007]$

From table 2, one can easily see that the classical method has calculated only fix point values, which are based on the classical mean or average formula for each interval of resistance with respect to both temperature and current. That's why we have found only a single value against graphene foam. It means that classical analysis is not reliable in making decisions and in concluding the solution of the problem. On the other hand, table 3 is expressing the neutrosophic analysis. From this table, it is seen that neutrosophic analysis is a more reliable analysis as it uses indeterminacy and gives the whole information about the variance of resistance at any specific

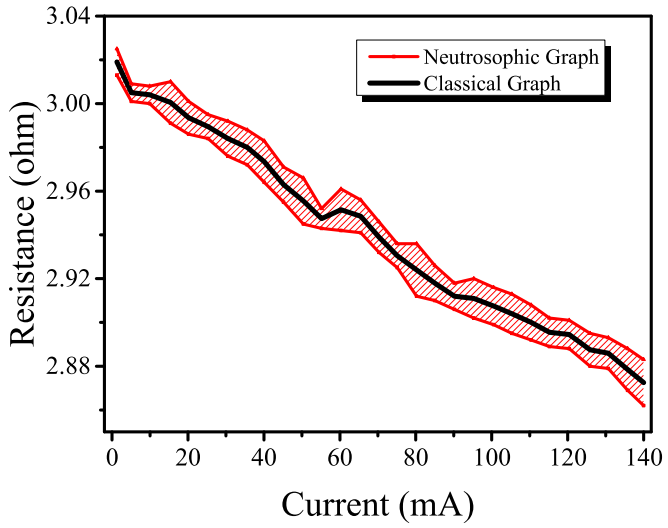

Figure 6. Graphs of resistance versus current for graphene foam.

value of temperature and current. For example, at 292 K temperature, the value of resistance calculated by the classical method is 3.036 Ω. But the neutrosophic method gives us a formula that is $R(292K)_N = 3.025 + 3.047I_N$ with an indeterminacy interval $I_N \in [0, 0.007]$. Which means that the value of resistance varies between 3.025 and 3.047 by putting the value of indeterminacy. Now let us see the graphical comparison of classical and neutrosophic analysis as shown in figures 5 and 6, respectively.

From the graphs, it is clearly seen that the resistance of graphene foam is decreasing as increases in temperature and current but not smoothly. Because graphene foam contains both conductor and semiconductor properties. Similarly, the graphs are also expressing the comparison between classical analysis and neutrosophic analysis. It is seen that graphs of classical analysis are not much flexible because these graphs are drawn at a fix point values. But graphs of neutrosophic analysis are shown more flexibility and more effectiveness to analyze the resistance of the graphene foam. Moreover, it is also seen that from a neutrosophic graph one can also analyze the classical graph. This is showing spuriousness of the neutrosophic method on the classical method.

4. Conclusions

The following work is based on the fabrication of the 3D graphene foam on Ni foam. The graphene is deposited on the Ni foam with the help of the CVD technique. The structural property of the graphene foam has been studied by the XRD technique, the surface morphology has been studied by FESEM, the quality of the graphene has been observed through the Raman spectroscopy and a specific surface area of about411.95 $m^2 g^{-1}$ has been measured through the BET technique. The resistance of graphene foam has been measured through the LCR meter and it is observed that the resistance has been decreased with an increase in temperature and current. Moreover, the analysis of the resistance has been performed by classical and neutrosophic analysis. And as the result, it is found that neutrosophic analysis is more informative and flexible to explain the resistance of the graphene foam.

Acknowledgments

The authors are deeply thankful to the editor and reviewers for their valuable suggestions to improve the quality and presentation of the paper.

Data availability statement

The data that support the findings of this study are available upon reasonable request from the authors.

Conflict of interest

None.

Funding

This study did not receive any funding in any form.

ORCID iDs

Muhammad Aslam https://orcid.org/0000-0003-0644-1950

References

Afzal U, Ahmad N, Zafar Q and Aslam M 2021 Fabrication of a surface type humidity sensor based on methyl green thin film, with the analysis of capacitance and resistance through neutrosophic statistics *RSC Adv.* **11** 38674–82
Afzal U, Alrweili H, Ahamd N and Aslam M 2021 Neutrosophic statistical analysis of resistance depending on the temperature variance of conducting material *Sci. Rep.* **11** 23939
Aslam M 2020a Design of the Bartlett and Hartley tests for homogeneity of variances under indeterminacy environment *Journal of Taibah University for Science* **14** 6–10
Aslam M 2020b On detecting outliers in complex data using Dixon's test under neutrosophic statistics *Journal of King Saud University-Science* **32** 2005–8
Aslam M 2021 Enhanced statistical tests under indeterminacy with application to earth speed data *Earth Sci. Inf.* **14** 1261–7
Aslam M 2021b A study on skewness and kurtosis estimators of wind speed distribution under indeterminacy *Theor. Appl. Climatol.* **143** 1227–34
Chen G, Liu Y, Liu F and Zhang X 2014 Fabrication of three-dimensional graphene foam with high electrical conductivity and large adsorption capability *Appl. Surf. Sci.* **311** 808–15
Chen H, Müller M B, Gilmore K J, Wallace G G and Li D 2008 Mechanically strong, electrically conductive, and biocompatible graphene paper *Adv. Mater.* **20** 3557–61
Chen J, Ye J and Du S 2017a Scale effect and anisotropy analyzed for neutrosophic numbers of rock joint roughness coefficient based on neutrosophic statistics *Symmetry* **9** 208
Chen J, Ye J, Du S and Yong R 2017b Expressions of rock joint roughness coefficient using neutrosophic interval statistical numbers *Symmetry* **9** 123
Christianto V, Boyd R N and Smarandache F 2020 *Three possible applications of neutrosophic logic in fundamental and applied sciences* (Infinite Study)
Dimchev M, Caeti R and Gupta N 2010 Effect of carbon nanofibers on tensile and compressive characteristics of hollow particle filled composites *Mater. Des.* **31** 1332–7
Ebrahimi S, Bordbar-Khiabani A, Yarmand B and Asghari M A 2019 Improving optoelectrical properties of photoactive anatase TiO2 coating using rGO incorporation during plasma electrolytic oxidation *Ceram. Int.* **45** 1746–54
Fasolino A, Los J and Katsnelson M I 2007 Intrinsic ripples in graphene *Nat. Mater.* **6** 858–61
Ferrari A C, Meyer J C, Scardaci V, Casiraghi C, Lazzeri M, Mauri F and Roth S 2006 Raman spectrum of graphene and graphene layers *Phys. Rev. Lett.* **97** 187401
Geim A K 2009 Graphene: status and prospects *Science* **324** 1530–4
Geim A K and Novoselov K S 2010 *The rise of graphene Nanoscience and technology: a collection of reviews from nature journals* (Singapore: World Scientific) 11–9
Huang X, Liu Y, Zhang H, Zhang J, Noonan O and Yu C 2017 Free-standing monolithic nanoporous graphene foam as a high performance aluminum-ion battery cathode *J. Mater. Chem. A* **5** 19416–21
Jiang W, Xin H and Li W 2016 Microcellular 3D graphene foam via chemical vapor deposition of electroless plated nickel foam templates *Mater. Lett.* **162** 105–9
Jinlong L, Meng Y, Suzuki K and Miura H 2017 Fabrication of 3D graphene foam for a highly conducting electrode *Mater. Lett.* **196** 369–72
Min B H, Kim D W, Kim K H, Choi H O, Jang S W and Jung H-T 2014 Bulk scale growth of CVD graphene on Ni nanowire foams for a highly dense and elastic 3D conducting electrode *Carbon* **80** 446–52
Qi J, Yan Y, Cai Y, Cao J and Feng J 2021 Nanoarchitectured Design of Vertical-Standing Arrays for Supercapacitors: Progress, Challenges, and Perspectives *Adv. Funct. Mater.* **31** 2006030
Qin B, Cai Y, Wang P, Zou Y, Cao J and Qi J 2022 Crystalline molybdenum carbide− amorphous molybdenum oxide heterostructures: *in situ* surface reconfiguration and electronic states modulation for Li− S batteries *Energy Storage Mater* **47** 345–53
Samad Y A, Li Y, Alhassan S M and Liao K 2015 Novel graphene foam composite with adjustable sensitivity for sensor applications *ACS Appl. Mater. Interfaces* **7** 9195–202
Smarandache F 2010 *The Neutrosophic Research Method in Scientific and Humanistic Fields*
Smarandache F 2013 *Introduction to neutrosophic measure, neutrosophic integral, and neutrosophic probability* (Sitech: Infinite Study)
Smarandache F 2014 *Introduction to Neutrosophic Statistics: Infinite Study* (Columbus, OH, USA: Romania-Educational Publisher)
Yan Y, Lin J, Cao J, Guo S, Zheng X, Feng J and Qi J 2019 Activating and optimizing the activity of NiCoP nanosheets for electrocatalytic alkaline water splitting through the V doping effect enhanced by P vacancies *J. Mater. Chem. A* **7** 24486–92
Yan Y, Lin J, Liu T, Liu B, Wang B, Qiao L and Qi J 2022 Corrosion behavior of stainless steel-tungsten carbide joints brazed with AgCuX (X = In, Ti) alloys *Corros. Sci.* 110231
Yang K and Guo J 2019 Three-dimensional nanoporous organic frameworks based on rigid unites *Mater. Lett.* **236** 155–8

Yavari F, Chen Z, Thomas A V, Ren W, Cheng H-M and Koratkar N 2011 High sensitivity gas detection using a macroscopic three-dimensional graphene foam network *Sci. Rep.* **1** 1–5
Ye J 2015 Improved cosine similarity measures of simplified neutrosophic sets for medical diagnoses *Artif. Intell. Med.* **63** 171–9
Zhang L L and Zhao X 2009 Carbon-based materials as supercapacitor electrodes *Chem. Soc. Rev.* **38** 2520–31
Zhang Z, Ding J, Xia X, Sun X, Song K, Zhao W and Liao B 2015 Fabrication and characterization of closed-cell aluminum foams with different contents of multi-walled carbon nanotubes *Mater. Des.* **88** 359–65